U. S. DEPARTMENT OF INTERIOR

U.S. GEOLOGICAL SURVEY

Audiomagnetotelluric Study of the Bursum Caldera and Mogollon Mining District, Southwest New Mexico

by

R.M. Senterfit, J.C. Ratté, R.J. Kamilli, and D.P. Klein

Open-File Report 96-037

1996

Audiomagnetotelluric Study of the Bursum Caldera and Mogollon Mining District, Southwest New Mexico

by

R.M. Senterfit, J.C. Ratté, R.J. Kamilli, and D.P. Klein

ABSTRACT

The geoelectric expression of part of the structural margin of the Bursum caldera was determined from three audiomagnetotelluric (AMT) profiles across the western part of the caldera in the Mogollon mining district. In this area, the structural and topographic caldera walls have been identified by detailed geologic mapping. The AMT profiles show that the caldera structural margin is associated with a resistivity exceeding 400 ohm-m caused by quartz veins, silicification of wall rocks, and (or) silicic intrusion in the caldera ring-fracture zone. Data were also acquired to the northeast and north of the Mogollon mining district, where the caldera margin is inferred to be buried by younger lava flows and volcaniclastic rocks. A resistivity anomaly near Negrito Mountain separates markedly different geoelectric sections, and shows high resistivity typical of silicic intrusions or silicified rocks.

In the gold-silver-copper producing Mogollon mining district, the Queen fault and vein, a reactivated caldera ring fault, is expressed as a high-resistivity anomaly (400 ohm-m or more) that is about 500 m wide and possibly extends to a depth of 1 to 2 km. Also at this depth, the resistivity decreases to less than 100 ohm-m for a width of about 500 m on both the east and west side of the vein. This symmetrical resistivity anomaly is centered in a 5-km-wide, 2-3 km deep, zone of 250-400 ohm-m that contrasts with resistivities exceeding 400 ohm-m on both sides. The observed pattern is interpreted to represent relatively low resistivity of variably intense propylitic alteration related to hydrothermal activity accompanying intrusion, silicification, or calcification in the Queen vein. The resistivity pattern becomes weak and incomplete 3 km north of the main area of mineralization within the Mogollon mining district, and disappears about 6 km to the north. The fault zone,however, is evident as a resistivity contrast. In the central part of the Mogollon mining area, the extent of the 250-400 ohm-m zone surrounding the main vein may represent the east-west horizontal extent of the hydrothermal system that produced the Mogollon mining area.

Two AMT traverses north of the Mogollon mining district did not positively identify the northern margin of the caldera, where it is covered by younger volcanic and volcaniclastic rocks. However, a major geoelectric discontinuity along one of the traverses and an associated resistivity high are best interpreted as a significant fault and an associated intrusion or silicified rock.

CONTENTS

Abstract ii
List of Figures..... iv
INTRODUCTION 1
DATA ACQUISITION AND PROCESSING 4
MOGOLLON AREA 8
Geologic relations 10
Section A-A' : Southern Mogollon Area 12
Section B-B' : Central Mogollon Area 17
Section C-C' : Northern Mogollon Area 19
Summary of Traverses A-A', B-B', C-C' 21
BEARWALLOW MOUNTAIN AREA 22
Section D-D' : Northeast Area 22
Section E-E' : North Area 27
CONCLUSIONS 29
ACKNOWLEDGEMENTS..... 31
REFERENCES 32

LIST OF FIGURES

Figure 1--Map showing outline of Bursum caldera and the location of audiomagnetotelluric (AMT) traverses.

Figure 2--Example of scalar AMT sounding data and depth-resistivity inversion using Bostick's method (Bostick, 1977).

Figure 3--Geologic map of Mogollon mining area showing AMT soundings on traverses A-A', B-B', and C-C'.

Figure 4--Depth-resistivity sections A-A', B-B', and C-C' across the Mogollon mining area.

Figure 5--Sounding curves for traverse A-A'.

Figure 6--Sounding curves for traverse B-B'.

Figure 7--Sounding curves for traverse C-C'.

Figure 8--Geologic map of the northwestern part of Bursum caldera showing AMT traverses D-D' and E-E'.

Figure 9--Alternative depth-resistivity sections for traverse D-D'.

Figure 10--Sounding curves for traverse D-D'.

Figure 11--Depth-resistivity section and sounding curves for traverse E-E'.

Audiomagnetotelluric Study of the Bursum Caldera and Mogollon Mining District, Southwest New Mexico

by

R.M. Senterfit, J.C. Ratté, R.J. Kamilli, and D.P. Klein

INTRODUCTION

An audiomagnetotelluric (AMT) survey was carried out in the spring of 1991 in an effort to identify the inferred but buried northern margin of the Bursum caldera north and east of the Mogollon mining district (Figure 1), in part because the margin is a possible gold and silver exploration target. Data from 51 AMT soundings (4.5-27,000 Hz) on five traverses were collected in the area of the Bursum caldera, Grant and Catron counties, southwest New Mexico (Senterfit and Abrams, 1991). Three of these were control traverses across the western margin of the caldera within the area of the Mogollon mining district about 20 km northeast of Glenwood, New Mexico. These traverses are located in the Mogollon Mountains, in the southwestern part of the Mogollon-Datil volcanic field. The control traverses were made to determine the electrical signature of the caldera boundary where the location of the caldera boundary is well defined and well exposed (Ratté, 1981). Two exploratory traverses were then made across the region of the inferred buried caldera margin north and east of the district to determine if the buried caldera boundary could be defined.

Although gravity and aeromagnetic data have been evaluated over parts of the Bursum caldera (Ratté and others, 1979, 1984), there have been no previous electrical resistivity studies. However, about 100 km northeast, in the northeastern part of the Mogollon volcanic field at the Ryan Hill area of the Sawmill Canyon caldera, resistivity was used to evaluate alteration patterns for the purpose of mineral assessment (Frischknecht and others, 1986). Also, about 100 km to the south-southwest, resistivity was employed to map the configuration of ring intrusions along the boundary of

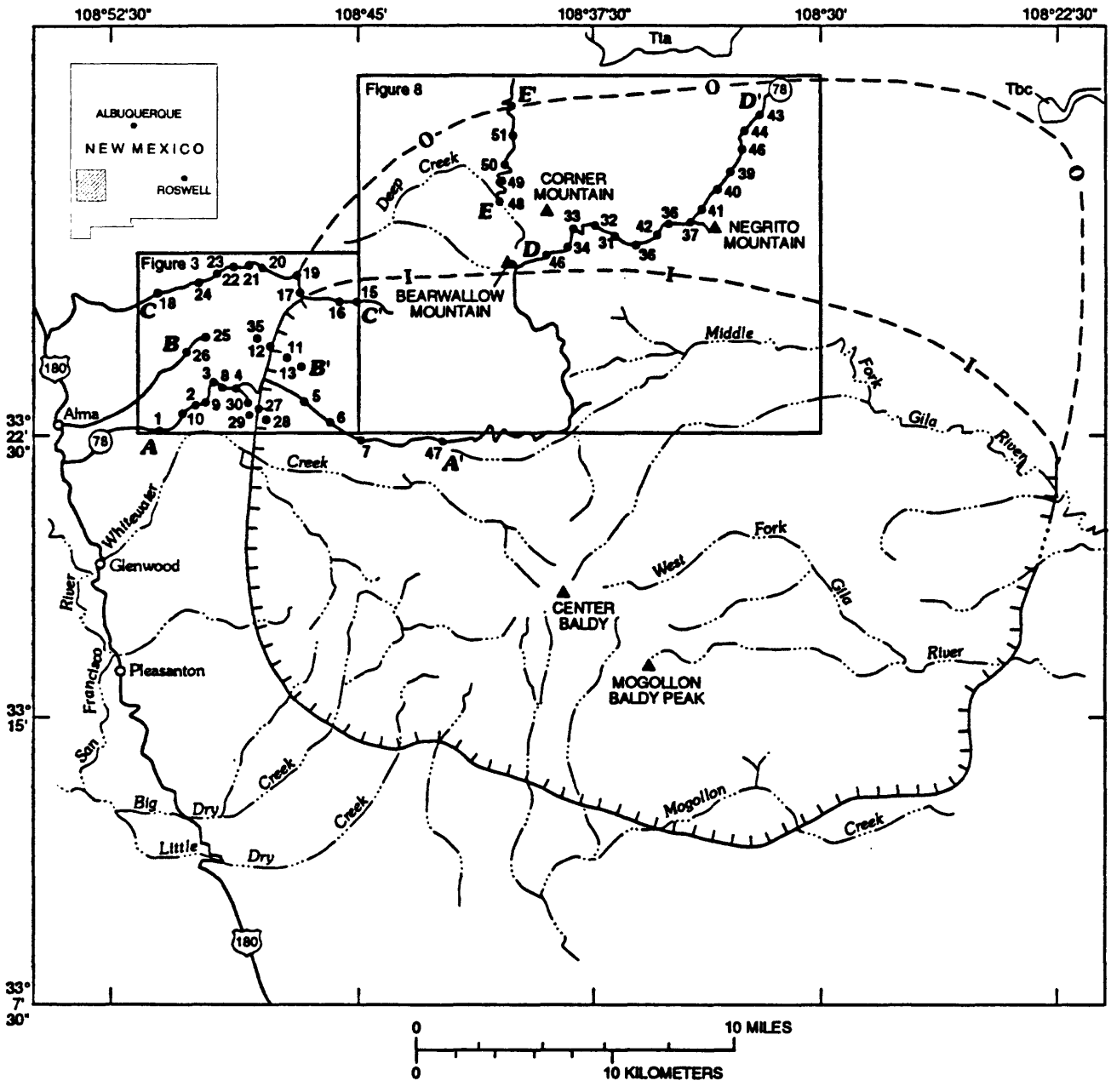

Fig. 1. Index map showing outline of Bursum caldera (hachured where known or approximately located), and inferred inner (I) and outer (O) limits of northern caldera margin-where obscured by younger rocks. Inner limit of caldera boundary is restricted by distribution of intracaldera Apache Spring Tuff on south side of Bearwallow Mountain (figure 3); outer limit is constrained by distribution of pre-caldera rocks north of the caldera, Tta (30.6) Ma andesite of Telephone Canyon, (same as porphyritic latite of Negrito Creek of Coney (1976, p.32, figure 1) and outflow Bloodgood Canyon Tuff, Tbc, (Richter and Lawrence, 1989; New Mexico Geological Society, 1982. Also shown: AMT sounding traverses A-A', B-B', C-C', D-D', and E-E' and locations of soundings 1-51 and outline of areas of figures 3 and 8.

Turkey Creek caldera (Senterfit and Klein, 1992). The AMT method was used in both of the investigations mentioned, and was selected for the present study because it is a rapidly deployed reconnaissance tool with maximum penetration of 2 to 3 km, which is appropriate for the study of shallow caldera structures.

The principles of the AMT method correspond to those of the magnetotelluric (MT) method (Vozoff, 1972), however the signals measured are at higher frequencies and originate mainly from atmospheric electrical disturbances rather than from ionospheric or magnetospheric phenomena (Strangway and others, 1973).

Resistivity in rock units is a sensitive function of pore-fluid and clay content, but is fundamentally independent of the silicate mineralogy (Keller and Frischknecht, 1966). One or a combination of the following conditions would be permissive, but not unique to,the electrical identification of the structural boundary of the Bursum caldera: 1) low-porosity ring intrusions or silicic hydrothermal deposits that would create a high resistivity, 2) ring faults that would provide contrasts of electrically distinct lithologic units, for instance altered air-fall tuff (low-resistivity) interbedded within well-welded and less-altered (high-resistivity) flow units faulted against resistive flow units or crystalline country rock, and 3) caldera ring fractures with associated brecciation, clay gouge, and alteration that would create low resistivity.

The geologic development of Bursum caldera has been reviewed by Ratté and others (1984). Bursum caldera is a resurgent, silicic ash-flow caldera about 40 km in diameter (Figure 1) that collapsed about 28 Ma following extensive eruption of rhyolitic tuff (Bloodgood Canyon Tuff). Subsidence continued during subsequent eruptions of Apache Spring Tuff (Oligocene), which accumulated entirely within the caldera. Subsidence occurred along a zone of ring fractures, which formed the original structural wall. The topographic wall, formed by the retreat of the original structural caldera wall by mass wasting, lies outside the structural wall and is well exposed in the western part of the Mogollon mining

district. Following collapse, resurgent intrusion was accompanied by internal doming, uplift, and renewed eruptions from ring-zone feeders, producing pyroclastic deposits, lava flows, dikes, and flow-banded rhyolites (including the Oligocene Fanney Rhyolite) on the western margin of the caldera. Basaltic andesites that erupted into the Bursum caldera moat both predate and postdate the ring-fracture rhyolites (Marvin and others, 1987) and cover most of the northern caldera boundary. The moat sequence also includes fluvial volcaniclastic sandstone and mudflow deposits.

The structural wall of the Bursum caldera is fairly well delineated for about 50- to 70-percent of the caldera, mainly on the southern and western caldera margins. On the north, much of the boundary of the caldera is buried beneath about 300-600 m of later andesitic lavas. The structural wall in the Mogollon mining area is inferred to have been reactivated during post-caldera basin and range extensional tectonism. Reconnaissance geologic mapping suggests that the trace of the northern margin of the Bursum caldera lies within a broad arcuate swath (the approximate innermost limits shown on Figure 1).

DATA ACQUISITION AND PROCESSING

The AMT data acquisition system (Hoover and others, 1976, 1978) records the time-varying amplitudes for two sets of orthogonal magnetic (H) and electric (E) fields. The receiver selectively filters and amplifies each of 16 frequencies distributed logarithmically across the range from 4.5 to 27,000 Hz. Resulting time-series are recorded as analog records. With the exception of the 14- and 27-kHz frequencies, which use navigation and communication signals of the very low frequency (VLF) band, the fields used are natural in origin. The primary source of observed AMT fields consists of distant atmospheric lightning activity (Strangway and others, 1973). The E-field sensors consist of two 25-m-long lines terminated with lead electrodes slightly buried in the Earth. The H-fields are sensed with a dual-axis, permalloy-

core induction coil system. For this survey, all measurements were made with the E- and H-sensors oriented north-south and east-west. Data were acquired in April and June of 1991.

Several simultaneous peaks from each pair of orthogonal E and H analog records were scaled and combined to compute an estimate of the scalar, magnetotelluric apparent resistivity, which is proportional to $[E_x/H_y]^2$, where x and y indicate perpendicular components (Vozoff, 1972, Strangway and others, 1973). Typically, 8 to 12 simultaneous samples of Ex and Hy are used to estimate an apparent resistivity at a given frequency. Two orthogonal measurements are made. We refer to the two estimated apparent resistivities as north-south (Rns) and east-west (Rew), according to the direction of the E-field measurement. An example of scalar AMT data along with it's Bostick inversion (Bostick, 1977) is shown in Figure 2. Most standard errors of these estimates range from 10 to 30 percent relative to the estimated mean (Senterfit and Abrams, 1991). Data with larger errors, or data that were inconsistent with the trend of other estimates have not been used. In addition, data records that yielded less than three simultaneous peaks were discarded. In the example shown in Figure 2, frequencies at 2,700 and 4,500 Hz are missing because of one or a combination of these criteria.

Derivation of depth-resistivity sections from the sounding curves (the logarithmic plot of apparent resistivities against frequency) was based on a one-dimensional (1-D) approximation such as used by Long (1985) and Frischkecht and others (1986). This approximation assumes that the resistivity of the earth is laterally uniform. The sounding data were averaged manually to produce a single, continuous, interpolated, and smooth curve that represents the logarithmic mean of the observed north-south and east-west apparent resistivity curves. A 1-D model of resistivity versus depth for each smooth curve was then derived using Bostick's transform (Bostick, 1977; Bostick and others, 1977; Goldberg and Rotstein, 1982).

The modeling procedure outlined above contains various

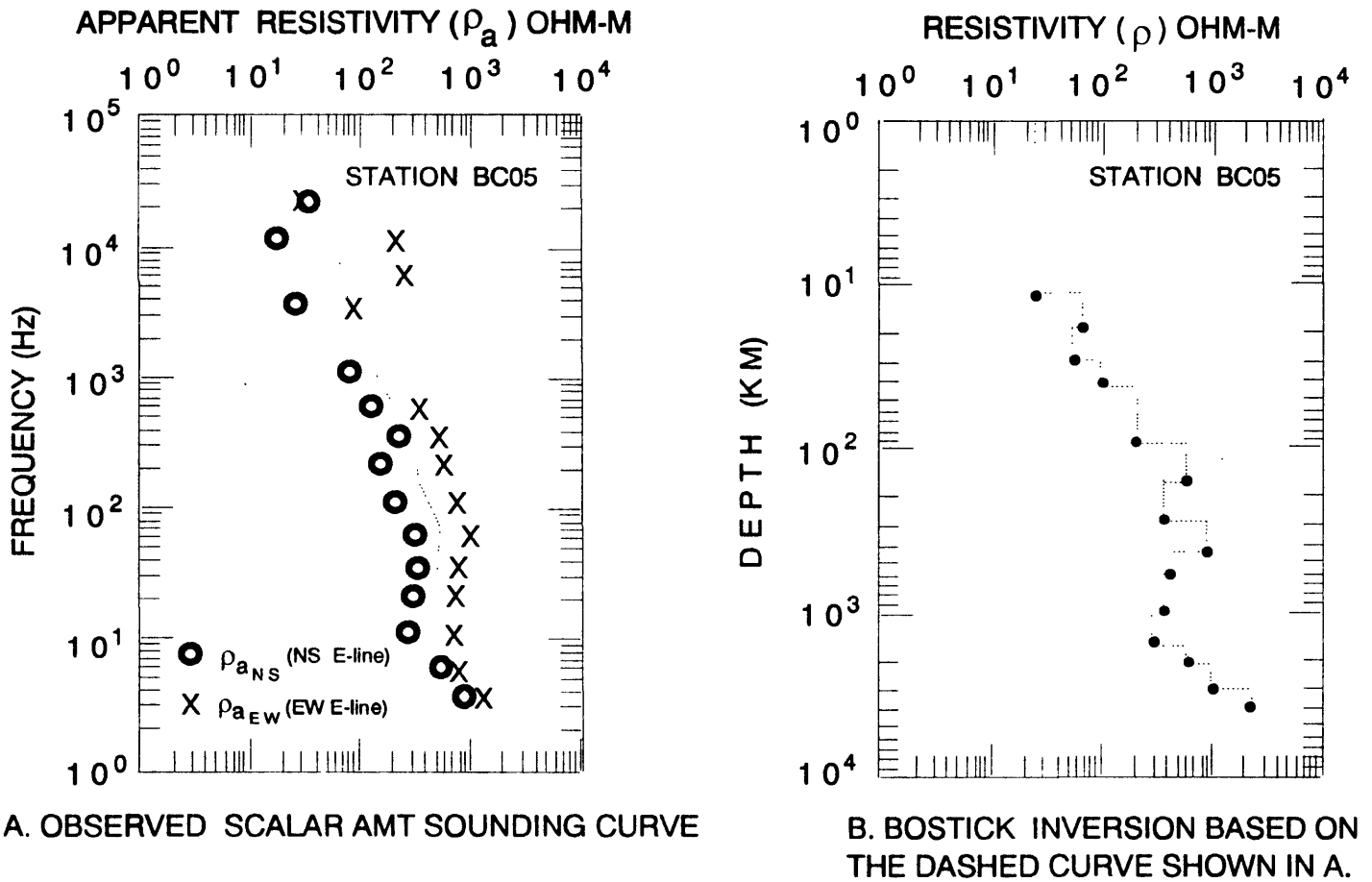

Figure 2--Examples of scalar AMT sounding data (A) and the depth-resistivity inversion using Bostick's method (Bostick, 1977) (B).

assumptions that relate to uncertainty in the results; we briefly comment on the assumptions inherent in establishing a smooth apparent resistivity curve based on the mean of separated apparent resistivity curves. Smoothness, although manually and qualitatively estimated, is an essential characteristic of electromagnetic induction data (Weidelt, 1972). Steep (greater than 45°) excursions of logarithmic apparent resistivity along the logarithmic frequency axis are assumed to reflect random noise or bias in the data, or possible 3-dimensional effects. Compared to random noise, bias in AMT data is more difficult to evaluate and remove. Bias may result from short wave length, natural- or cultural-source fields, or errors in instrument calibration factors. Nearby topography or shallow (a depth of a few meters) resistivity inhomogeneities may also be significant sources of geologically biased curves that can severely distort the interpretation of deeper electrical structure (Jiracek, 1990).

The use of the logarithmic mean for modeling scalar AMT data was standardized by Strangway and others (1973), Strangway and Kozier (1979), and Hoover and others (1976). If the electrical structure is one-dimensional, then both curves coincide and averaging simply removes random noise or averages bias. In most soundings described here,the two curves and their random-noise envelopes are separated, which indicates a 2- or 3-dimensional electrical structure, anisotropy in either structural or grain domains, or bias. We assume that non-geologic bias is unimportant. The implicit justification for using a mean curve in 2- or 3-D electrical environments is the inherent uncertainty in the principle axes (oriented parallel and perpendicular to electrical strike; Vozoff, 1972) for scalar AMT data. This axis cannot be defined with scalar data, and there is equal but unknown uncertainty in attempting to interpret the maximum, the minimum, or the mean curve. However, if the observation coordinates are along the MT principal axes of a 2-D electrical structure, then the logarithmic mean of apparent resistivity curves (equivalent to the logarithm of the geometric mean) is a tensor invariant curve

(Berdichevsky and Dmitriev, 1976; Eggers, 1982; Park and Livelybrooks, 1989) and provides a consistent curve for interpretation that will correspond to the invariant curve from tensor MT data. Furthermore, if geological information allows an inference concerning the electrical strike, and observations are made in the coordinate system of this strike, then 2-D modeling that attempts to simultaneously fit the maximum and minimum curves of scalar data may be justified.

To display the resistivity structure, the 1-D models from individual soundings were composited along various profiles and contoured to provide approximate depth-resistivity sections. Contour intervals of logarithmically equal values are used. On each of the cross sections, station locations are perpendicular projections to a straight line from the sounding location. We have drawn a vertical line below each sounding to indicate the depth of penetration. Five cross sections form the basis of subsequent interpretation. Because the cross sections are based on 1-D modeling, some distortions may be present in the displayed resistivity structure. These distortions are more severe where the resistivity changes rapidly along section relative to the depth of penetration and where the data show large separations between the maximum and minimum curves. However, the major features shown on the sections probably provide a first-order indication of subsurface conditions.

MOGOLLON AREA

Depth-resistivity cross sections in the Mogollon mining district, based on the three AMT traverses, are represented by profiles A-A',B-B, and C-C (Figure 3). The sounding stations are projected perpendicularly to the lines of profile, and thus the horizontal distances between soundings along the profiles are distorted. This presentation has the advantage that spatial relations across the area are displayed, allowing comparison of north-south variations between the three traverses. The sections

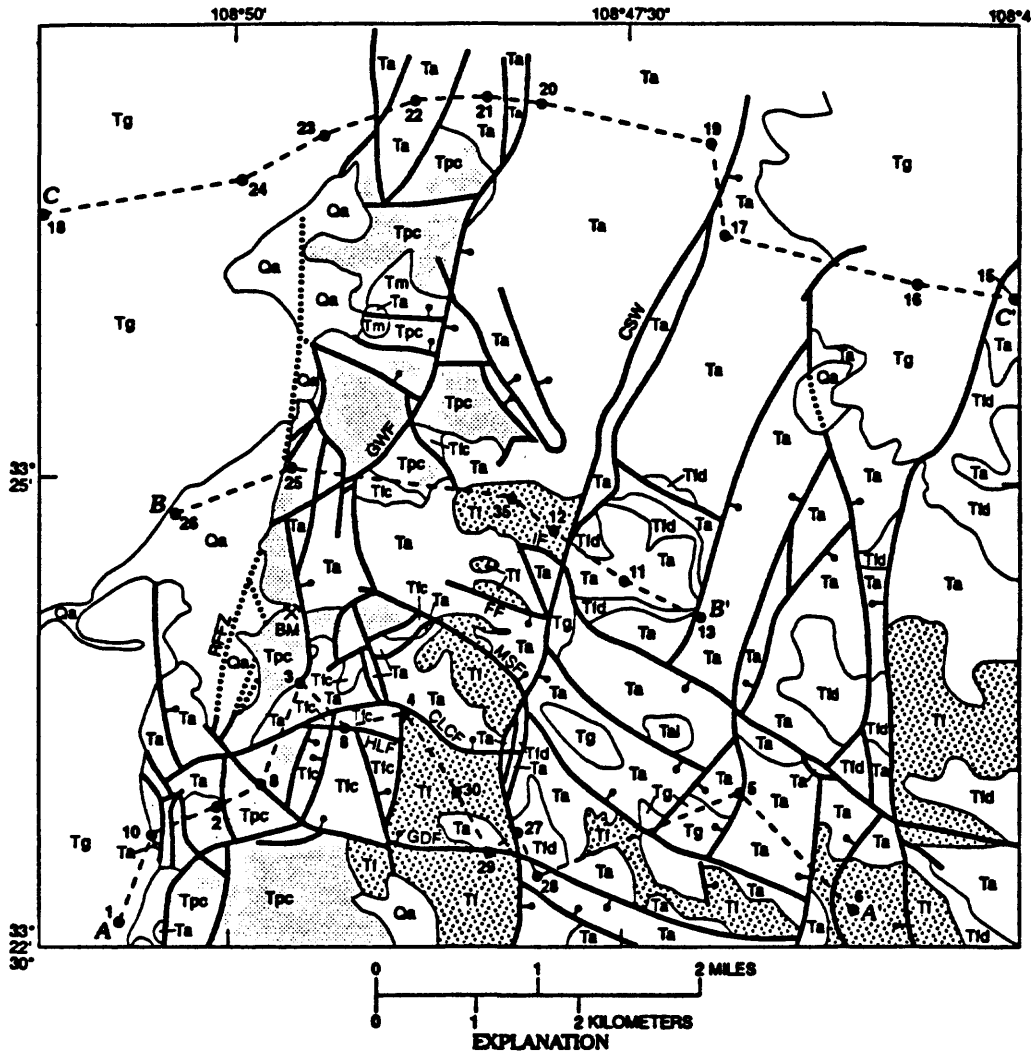

Fig. 3. Geologic map of Mogollon mining area showing AMT soundings on traverses A-A', B-B', and C-C'. AMT soundings are shown by numbered dots. Geology after Ratte' (1981) as modified from Ferguson (1927). Most of the stations are on established roads and are projected to profiles A-A', B-B', and C-C'.

in Figure 3 all cross the Queen fault and vein system which has been interpreted as the structural wall of the Bursum caldera (labelled CSW in Figure 3.)

Geologic relations

Ferguson (1927) provided the first comprehensive study of the Mogollon mining District. More recent geologic maps (Ratté, 1981; Ratté and Gaskill, 1975) focus on the regional aspects of the area. Ratté and others (1984) have provided a summary of many broad-scale features of the Bursum caldera.

The caldera structural wall is defined by the juxtaposition of the pre-caldera volcanic sequence (Tpc in Figure 3) and the caldera filling tuff, and breccias from the caldera wall. Exact location of the structural wall can be difficult, particularly if resurgent doming of the central caldera block has created a moat between the eroded topographic caldera wall and the resurgent dome, and if the structural wall is buried beneath younger moat-filling volcanic rocks and volcaniclastic sedimentary rocks.

Within the Mogollon mining district (Figure 3) the structural wall most likely is not a single fault but rather a complex combination of stepped faults (Ratté and others, 1989). However, the main caldera fault probably is the Queen fault and vein system as constrained by the easternmost outcrops of pre-caldera rock (Cooney Tuff, Tpc), which is the oldest rock exposed in the caldera wall. On the surface, Cooney Tuff is separated from the Queen fault only by ring-fracture intrusions and extrusive rocks (Fanney Rhyolite, Tf) and other moat deposits. The Queen fault is interpreted to have at least 350 m of displacement, down to the east (Ratté, 1981; Ferguson, 1927.)

The Queen fault, though probably coincident with the main caldera structural wall, offsets post-caldera moat deposits, and thus is interpreted as a reactivated fault. North of the area shown in Figure 3, the Queen fault continues northward and thus departs from the inferred caldera structural wall. Other major faults that parallel the Queen fault include the Great Western

fault (GWF, Figure 3) and the range-front fault-zone (RFFZ, Figure 3). The location and nature of the range-front fault-zone, generally inferred to be a basin and range fault with displacement of 350 to 1,000 m, down to the west (Ratté, 1981), is poorly constrained by surface or subsurface evidence.

Hydrothermal alteration and veining in the Mogollon mining district is largely confined to, but not restricted to, the rectangular area that is bordered by the principal faults of the area. These include the Queen and Great Western faults, on the east and west sides of the district, respectively, and the Gold Dust and Independence faults on the north and south sides, respectively. All ore produced has been from the Queen fault and to the west,principally from the Confidence-Last Chance, Maud S, and Fanney structures, between AMT traverses A-A′ and B-B′.

Ore minerals in the district include electrum, argentite, mckinstryite, tetrahedrite, chalcopyrite, and bornite. Veins are predominantly massive quartz, chalcedony, and(or) calcite, with total sulfides commonly less than 2 volume per cent. The veins, as wide as 20 m, are located mainly along the north-south striking Queen fault and several west-northwest-striking fault or fracture systems. Deposits of the Mogollon mining district are of the Comstock epithermal vein type of deposits (Mosier and others, 1986), which are generally characterized by their quartz-adularia-sericite alteration, low sulfide content, and relatively low chlorite content compared, for instance, to deposits at Creede, Colorado (higher chlorite), and Goldfield, Nevada (higher sulfide). Recent $^{40}Ar/^{39}Ar$ dating of vein adularia (W.C. McIntosh, oral comm., 1990) confirms K-Ar ages (Ratté and others, 1983) that indicate that the veins were deposited about 17 Ma, well after caldera development. Cumulative production from the Mogollon district included 22 million ounces Ag and 450,000 ounces Au (an average grade of 10 oz./ton for Ag and 0.2 oz./ton for Au), 886,000 lbs Cu, and 14,000 lbs Pb (Ferguson, 1927).

Country rock consists of a variety of mostly mid-Tertiary volcanic and volcaniclastic rocks, locally overlain by Tertiary

sedimentary rocks that are generally moderately well cemented (Gila Formation, Tg, Figure 3), and Quaternary alluvium. The mid-Tertiary volcanic rocks are typically pervasively propylitized. The volcaniclastic and pyroclastic rocks, including the pyroclastic Deadwood Gulch Member (Tfd, Figure 3) of the Fanney Rhyolite are prone to alteration and weathering to clay minerals. By contrast, the intrusive Fanney Rhyolite is quite fresh in most places, but may be silicified or argillized locally.

The intensity of alteration has a profound affect on rock resistivity. Resistivity is largely controlled by wet pore space and the availability of rock material with enhanced ion exchange capability, such as clays (Keller and Frischknecht, 1966, p.23; Nelson and Anderson, 1992). Resistivity decreases significantly with small increases in ionic fluids or clay content in the rock. No detailed study of alteration within the Mogollon mining area has been conducted, but epithermal systems are typically characterized by intense silicic and carbonate alteration in the central part of the vein system, which is bordered by a zone of intense argillic alteration grading outward into propylitic alteration (Allis, 1981; Buchanan, 1981; Heald and others, 1987; Irvine and Smith, 1990). The argillic (kaolinite-illite) is known (Buchanan, 1981) in the Mogollon district, but propylitic (montmorillonite-chlorite) alteration is more common, is pervasive in the andesites, and tends to increase in intensity toward the veins. Drill cores from the Mogollon district reveal highly silicified breccias throughout much of the mining area and major sills of high-silica (Fanney Rhyolite) rock. The extent of vertical feeders into these sills is unknown, but, if widespread, combined more highly resistive sills and dikes may significantly increase the resistivity of large volumes of clay-bearing alteration sampled by AMT soundings.

Section A-A′: Southern Mogollon Area

Section A-A′ (Figure 4, bottom) extends from the sedimentary basin (stations 1 and 10) west of the range-front fault zone, eastward into a zone of pre-and post-caldera rocks, and across the

exposed ring-fracture zone and Queen fault to station 6, which is located toward the inner margin of the caldera moat. Parts of this section are in an area where the subsurface geology is known because of extensive mining and core drilling. AMT sounding curves for this traverse are shown on Figure 5.

Low resistivity values (less than 100 ohm-m) characterize rocks from station 1 to station 4. Such values can be attributed to volcaniclastic rocks (Gila Formation) or fractured and weathered near-surface rocks. The thickness of the low-resistivity zone decreases toward the east, from station 1 to station 4, probably because the surface and near-surface rocks are less fractured.

Stations 10 and 2 are within the range-front fault zone. The fault zone may be about 1 km wide and comprise several discrete, subparallel faults, an interpretattion based on fault exposures in the Bearup mine (BM in Figure 3) about 2 km north of line A-A'. A fault in the Bearup mine exposes clayey gouge rich in chlorite- and calcite-coated slickensides 74 m wide.

At station 2, resistivity values of 250 and 400 ohm-m are higher than at comparable levels below stations 9 and 10, immediately to the east and west, respectively. This is not an electrical signature of a wide, clay-rich fault zone. If we assume that the fault zone has a consistent clay-rich character along strike, then the ratio of the conductive fault to the resistive host rock must be too small for resolution by the AMT method. The high may then represent a lithologic variation related to either lower porosity or variable alteration. If the lithologic characteristics of the range-front fault zone change along strike, for instance, if they show silicification or calcification instead of clay-gouge, then the data may be sensing a resistive zone directly attributable to the fault zone. Ratté (1981) mapped calcite veining in a splay of a fault 200 m to the southeast of station 2, but, although the area surrounding station 2 appears to be pervasively faulted, there are only two indications of calcite veining on Ratté's map (1981). Additional data are required to explain this anomaly.

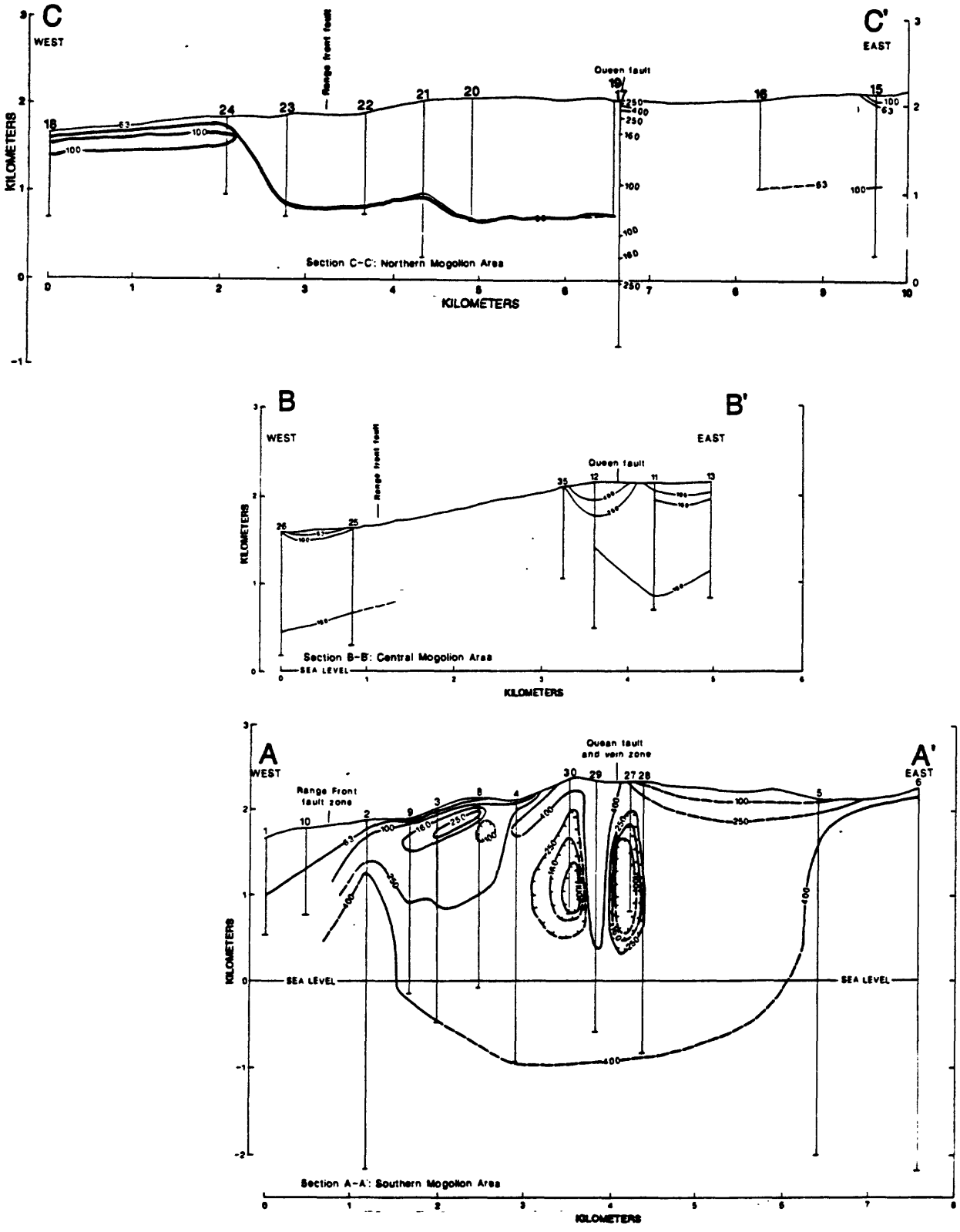

Fig. 4. Depth-resistivity sections A-A', B-B', and C-C' across the Mogollon mining area. Sections are based on contouring the results of 1-D inversion of the geometric average of the minimum and maximum curves for each sounding. Contours are in ohm-m, with roughly equilog contour intervals.

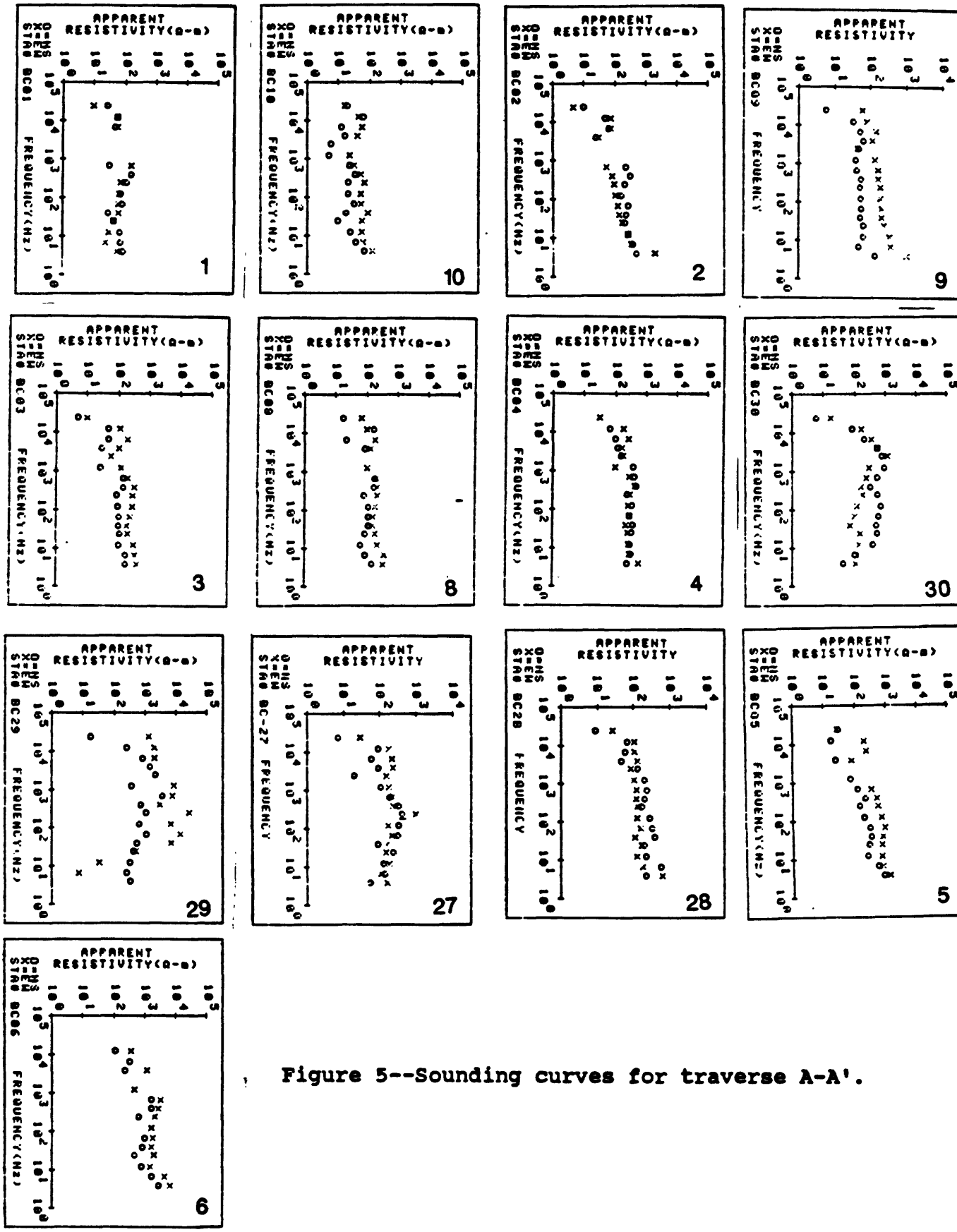

Figure 5--Sounding curves for traverse A-A'.

At station 3, a high-resistivity zone (250 ohm-m) is present at a depth of about 150 m and appears also (160 - 250 ohm-m) at stations 9 and 8. Ferguson's map (plate 11, 1927) shows a fault within about 30 m of station 3. Ferguson also showed this fault to be silicified and(or) calcified and mineralized about 500 m to the north, where it hosts the Bearup mine. This unnamed fault, exposed at station 3, is believed related to high resistivity rocks between stations 9 and 8.

Station 8 is on the Hard Luck fault that Ferguson (1927, plate 11) mapped as mineralized but nonproductive. The small low resistivity interval (less than 100 ohm-m) between depths of 300 m and 500 m is within the noise level of the inversions.

At Station 4, the Confidence-Last Chance vein-fault system (CLCF, Figure 3) follows the fault contact between Apache Spring Tuff (Tpc) on the south and Mineral Creek Andesite (Ta) on the north. Station 4 is located directly on the Confidence-Last Chance fault/vein (Figure 3), and also on a part of the vein that has been extensively stoped out at a depth of about 500 m (Ferguson, 1927, plate 21). The stoped zone, or the resistive fault zone itself, may be responsible for the increased resistivity at about 500 m depth.

The primary feature of section A-A' is the large resistivity anomaly associated with the Queen fault and vein system (stations 30, 29, 27, and 28, Figure 4 bottom). Stations 30 and 29 are about 500 m to the west of the Queen vein and stations 27 and 28 are about 250 m to the east of the Queen vein (Figure 3). The contour pattern (Figure 4, bottom) shows symmetry relative to station 29 that could be interpreted as a central silicified zone, bordered by clay-altered rock. An alternative factor to be considered is the high-resistivity (greater than 400 ohm-m) Fanney Rhyolite (Tf, Figure 3) found within and west of the Queen fault/vein system in this area. This high-resistivity Fanney Rhyolite contrasts with the incompetent pyroclastic rock (Deadwood Gulch Member, Tfd, Figure 3) and the younger but more altered andesites (Mineral Creek Andesite, and Last Chance Andesite; both Ta, Figure 3) to the east. The difference in lithology of rocks across the vein and fault zone

is apparent in the topography; the zone is marked by a cliff in many places.

Cross section A-A′ (Figure 4, bottom) suggests that the high resistivity associated with the Queen vein extends to a depth of about 2 km beneath stations 29, with vertically elongate, low-resistivity zones extending to a depth of about 1.5 km on either side of the Queen vein zone. The effect of static offset in AMT data is to extend near-surface resistivity contrasts to depth (Jiracek, 1990); we may be visualizing such an effect in Figure 4. The true two-dimensional geometry is probably distorted significantly in this area of large, abrupt, and rapid resistivity contrasts that overemphasize anomalies.

The deep 400 ohm-m contour, which indicates resistive basement, is detected only on the western and eastern parts of traverse A-A′ (stations 2,3,5,6). Excluding the shallower parts of silicified veins, resistive (greater than 400 ohm-m) rock is at least 2 km deep in the central part of the traverse. If the disappearance of high-resistivity rock results from regional propylytic alteration, the width of the hydrothermally altered zone along this traverse is about 5 km. This width corresponds well with known geology.

Section B-B′: Central Mogollon Area

Traverse B-B′ (Figure 3) extends from the alluvial basin (station 26) southeastward across the Queen fault and vein (between stations 12 and 11) to station 13, located in the eastern part of the moat several kilometers west of the resurgent dome of the caldera. Figure 4 (middle) shows the resistivity-depth section. Figure 6 shows the sounding curves for this section.

Low resistivities (less than 100 ohm-m except at sounding 12) in most of this section are consistent with the lack of fresh silicic rock such as Fanney Rhyolite (Tf, Figure 3) or major vein silicification or calcification along the traverse. Station 25 is about 300 m west of the range-front fault, yet shows little resistivity increase compared to station 2 in section A-A′.

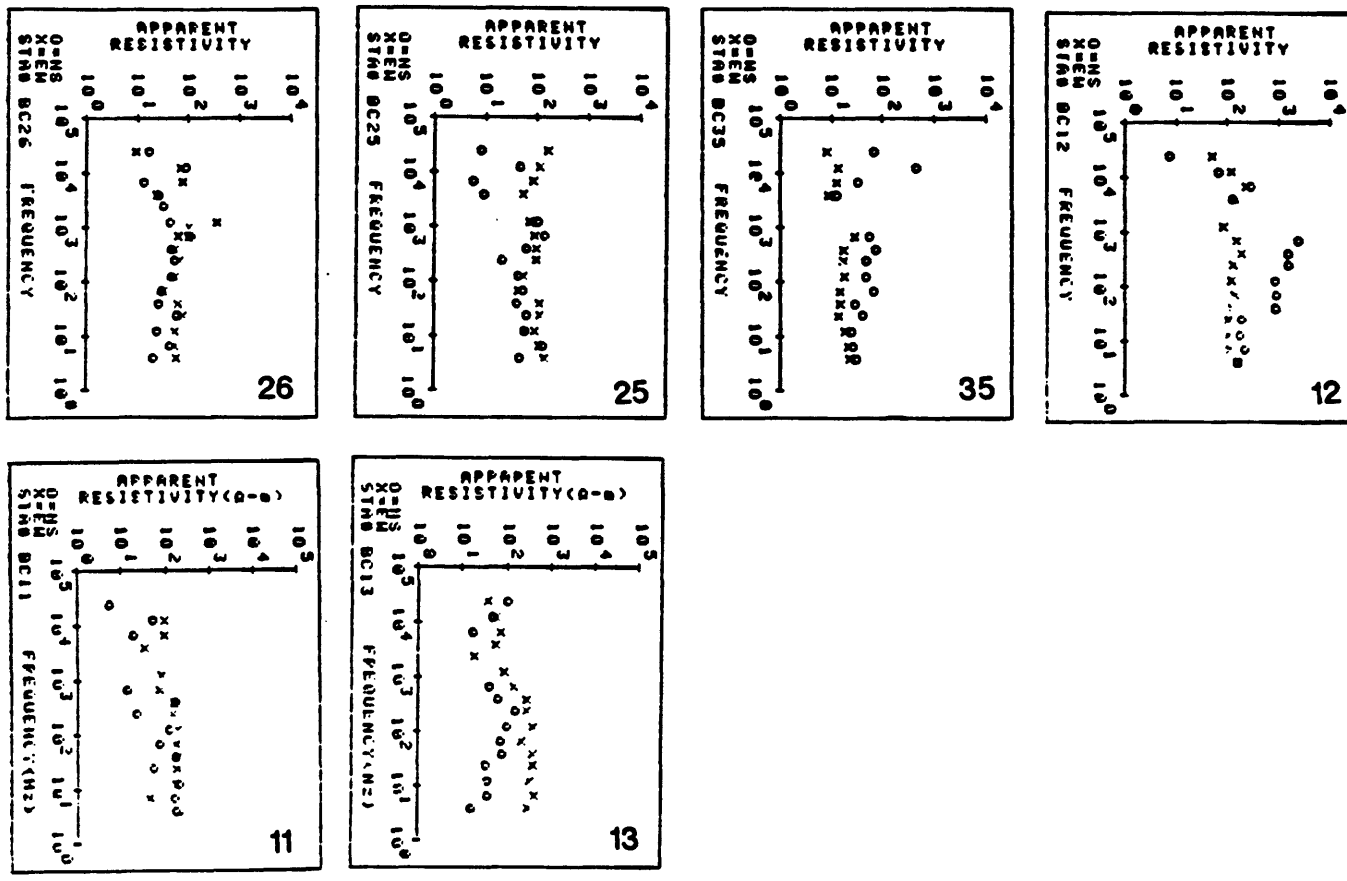

Figure 6--Sounding curves for traverse B-B'.

Stations 35 and 12 are on Fanney Rhyolite (Tf, Figure 3), but only sounding 12 shows significant increased resistivity. Sounding 12 is about 300 m west of the Queen vein, for which drill-hole data indicate that it is mineralized to a depth of nearly 400 m. The depth of the contact of Fanney Rhyolite with underlying Mineral Creek Andesite (Ta, Figure 3) is also known from numerous diamond drill holes in the area. At station 12, resistivity greater than 400 ohm-m extends from the surface to a depth of nearly 350 m, which is consistent with the extent of known vein development, and within 100 m of the base of the Fanney Rhyolite. Inasmuch as sounding 35 shows a fairly constant resistivity of 100 ohm-m (Figure 5), we believe that veining and silicified wall rock are the chief causes of enhanced resistivity at sounding 12.

Section C-C′: Northern Mogollon Area

Traverse C-C′ (Figure 3) is the northernmost profile in the Mogollon area and north of any known economic mineralization. The resistivity-depth section is shown at the top of Figure 4. Sounding curves for traverse C-C′ are shown on Figure 7.

The traverse begins on Gila Formation (Tg, Figure 3), west of the Mogollon Range (station 18) and extends eastward across the range-front fault without significant AMT expression (Figure 4, top; between stations 23 and 22). The section continues over Last Chance Andesite and its equivalents (Ta, Figure 3), across the Queen fault (between stations 19 and 17) to station 15 in the caldera moat, 4-5 km west of the resurgent dome. Sounding 16 on C-C′ is on an inlier of Gila Formation (Tg, Figure 3). Low resistivity (less than 100 ohm-m) is ubiquitous along the section (Figure 4 top) with the exception of a thin layer below soundings 18 and 24 and at sounding 17 on the east side of the Queen fault zone.

Between stations 18 and 24 in the sedimentary basin, a resistive zone of 100-250 ohm-m is present from a depth of about 125 m to about 260 m (Figure 4, top). The presence of a resistive layer within sedimentary rocks may include: 1) a lava flow, 2) a

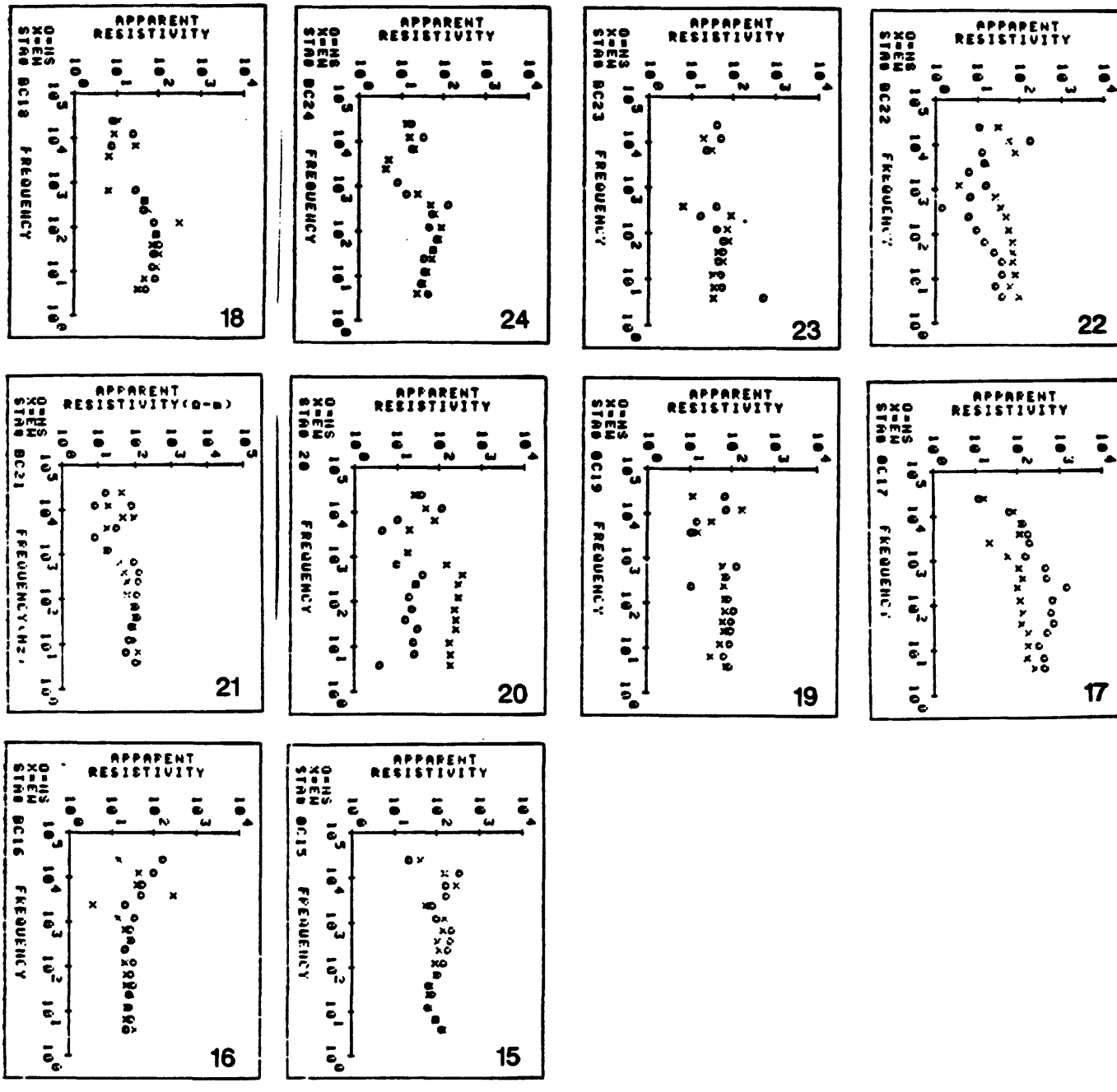

Figure 7--Sounding curves for traverse C-C'.

layer of clean sand and gravel interbedded between more clay rich layers, or 3) a zone of carbonate cementation. This horizontal zone could correspond to the basalt flows of Harve Gulch (Houser, 1981) which crop out about 7 km to the southwest in the San Francisco river valley in the Alma Quadrangle. A 200-m deep water well (Copper Creek well) about 1 km south of station 18, encountered no basalt (Brenda Houser, oral communication, 1991). However, any of the three alternatives listed may be quite limited in area, and, therefore, without further data, we cannot favor one alternative over another.

At station 17, high resistivity values (250-400 ohm-m) are present in the upper 100 m of the section (Figure 4, top). This station is located less than 100 m east of the Queen fault and vein system. The nearest sounding west of the fault, sounding 19, is offset about 0.7 km north of 17 (Figure 3). The Queen fault and vein system in this area is composed of massive quartz and calcite lamellae, which should be resistive. For soundings offset from a resistive vein, the component that would be increased is the perpendicular E-field (in this case the Eew). At station 17, the maximum is Ens and the minimum is Eew, with a separation in apparent resistivities (Ens vs. Eew, Figure 7) of about a log-cycle. The shift in the Ens component is scattered and inconsistent with a resistive dike to the west or east of the sounding. The minimum curves (Eew) at both stations are almost coincident, and the minimum and maximum are coincident at station 19. The contours shown (Figure 4, top) might be the result of noise on the Ens sensor at sounding 19, although the possibility of buried, shallow veining transverse to the Queen fault cannot be ruled out.

Summary of Traverses A-A′, B-B′, and C-C′

Traverses (A-A′, B-B′, C-C′) were established largely to identify the signature of a caldera structural margin in a known environment. The data for traverses A-A′ and B-B′ suggest that either the caldera margin where inferred to coincide with a silicic

ring intrusive and extrusive rock or a vein system may show distinctively high resistivity. Traverse C-C′ crossed the caldera margin where weak veining is known but where ring dikes have not been mapped. This traverse showed little evidence for a resistivity contrast indicating either the caldera margin or the vein-system in that part of Bursum caldera.

BEARWALLOW MOUNTAIN AREA

AMT traverses D-D′ and E-E′ were chosen to cross the area where the inferred northern margin of the Bursum caldera is buried beneath younger rocks, mainly lava flows of Bearwallow Mountain Andesite (Figure 8). The caldera margin is constrained by geologic mapping to be located north of outcrops of Apache Spring Tuff, which fills out the caldera, and south of pre-caldera rocks, which crop out just north of the area shown in Figure 8.

Section D-D′: Northeast Area

Traverse D-D′ runs north-northeast about 15 km, from station 46, just east of Bearwallow Mountain, past Negrito Mountain to station 43 (Figure 8). Bearwallow Mountain Andesite crops out or is present as float along most of the traverse (stations 46 to 40) and is estimated to range between 100 and 300 m thickness. The northeast part of the traverse crosses volcaniclastic sedimentary rocks (Tgb) and post-caldera rhyolite lava flows (Tr). The rhyolite flows could be related to the Bursum caldera ring-fracture zone.

Resistivity cross sections for AMT traverse D-D′ are shown in Figure 9, and sounding curves for traverse D-D′ are shown in Figure 10. Whereas the resistivity sections for traverses A-A′, B-B′, and C-C′ are based on the average of the minimum and maximum resistivity curves for each sounding, the sections for traverse D-D′ have been modelled for both the averaged apparent resistivities (Figure 9a) and for the minimum apparent resistivities (Figure 9b). Where the separation between the maximum and minimum apparent

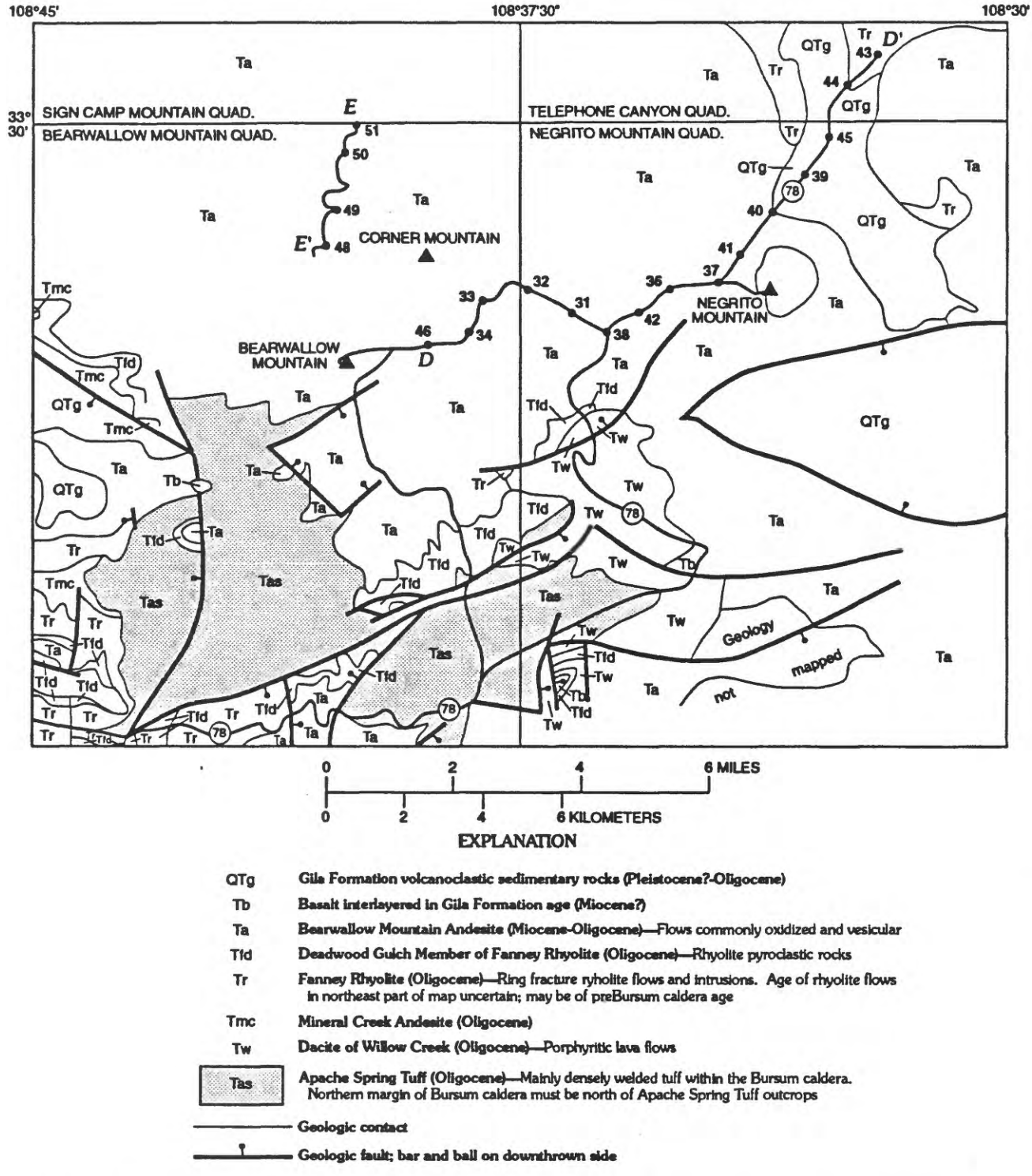

Fig. 8. Geologic map of the northwestern part of Bursum Caldera showing AMT traverses D-D' and E-E'. The AMT soundings (numbered dots) were acquired to attempt to detect the north margin of the caldera in this area where its location is unknown. Geology modified from Coney, 1976. Most of the stations are located on established roads and are projected to profiles D-D' and E-E'.

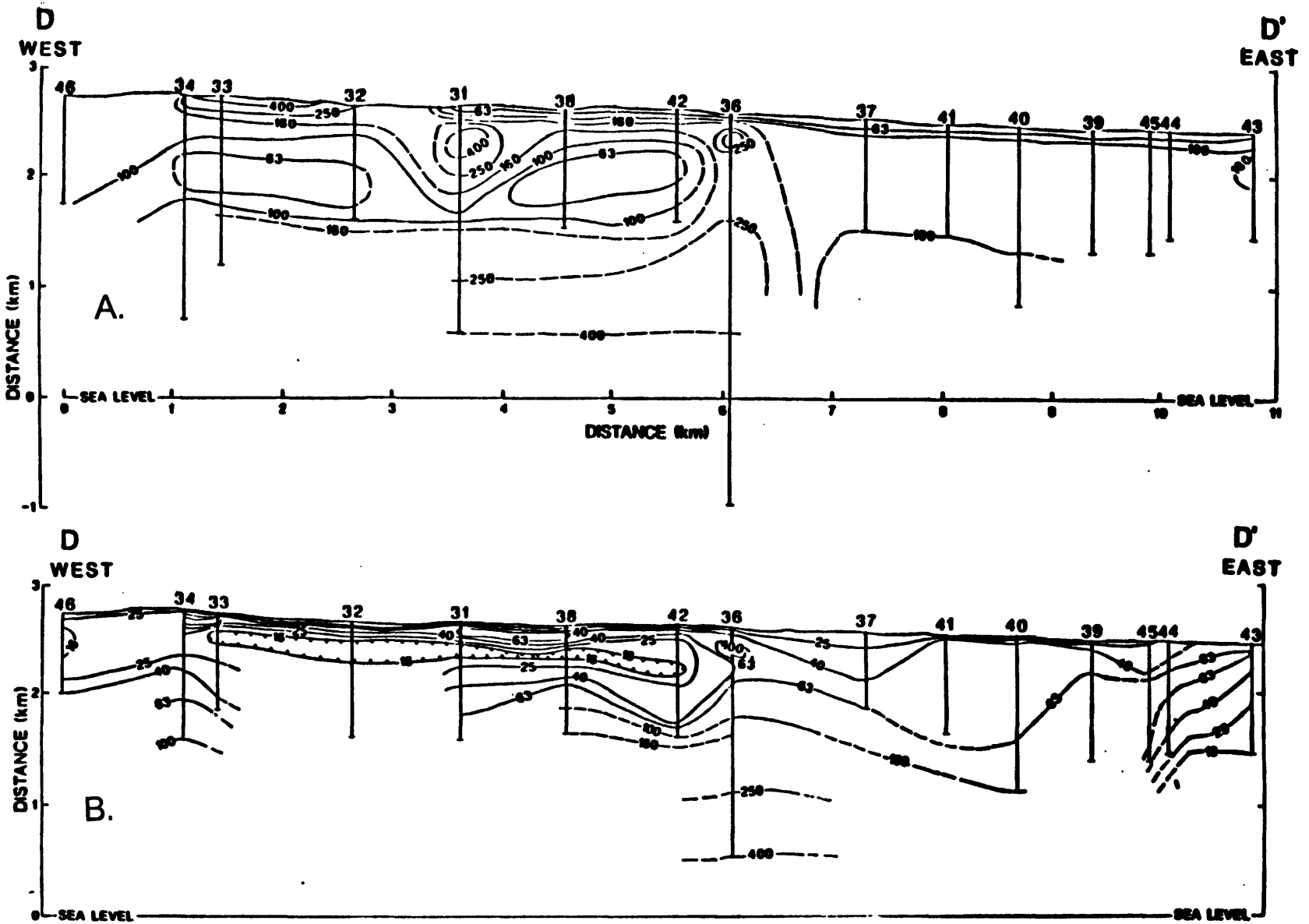

Figure 9--Alternative depth-resistivity sections for traverse D-D'. a) Contours based on the geometric average of the minimum and maximum sounding curves (see explanation with Figure 4). b) Contours based on the minimum resistivity curves for each sounding.

resistivity is appreciable, the separation is essentially constant with frequency. Such frequency-independent separation, or static shift (Jiracek, 1990), is characteristic of lateral resistivity contrasts at or near the surface and could represent variations in the resistivity structure caused by highly weathered rocks in the upper few tens of meters of the soundings, rather than inhomogenieties in the underlying rock sequence. Thus, the minimum resistivity curves may be a better estimate of the resistivity section than the averaged curves in this instance.

Both the averaged and minimum sections for traverse D-D' show a resistivity discontinuity at station 36. Relatively high resistivities beneath the stations west of station 36 are in contrast to generally lower resistivities, increasing monotonically with depth, northeast of station 36 (Figure 10). Northeast of station 36, both sections (Figs. 9a,9b) show resistivity values that are generally less than 100 ohm-m to a depth of about 1.5 km, indicating an electrically homogeneous rock sequence east of the discontinuity. However, local zones of 160-250 ohm-m are present in the averaged resistivity section beneath stations 40 and 43 (Figure 9a). Station 40 is at the contact between Bearwallow Mountain Andesite and overlying volcaniclastic sediments; station 43 is on rhyolite lava flows at the end of the traverse.

Both sections (Figures 9a,9b) show more complicated resistivity patterns west of station 36. The section with averaged resistivities (Figure 9a) has a 400 ohm-m resistivity high bounded by resistivity lows of less than 63 ohm-m beneath station 31, but this anomaly is absent on the minimum resistivity section (Figure 9b).

Marked similarity in shape and amplitude of all resistivity curves from station 36 west to station 46 (Figure 10), irrespective of the degree of separation of the curves, indicates a consistent rock sequence beneath these stations. The minimum resistivity section (Figure 9b) for this part of the traverse shows a low resistivity zone (less than 25 ohm-m) beneath stations 33-42 at a depth of about 200 m, which is interpreted as a zone of

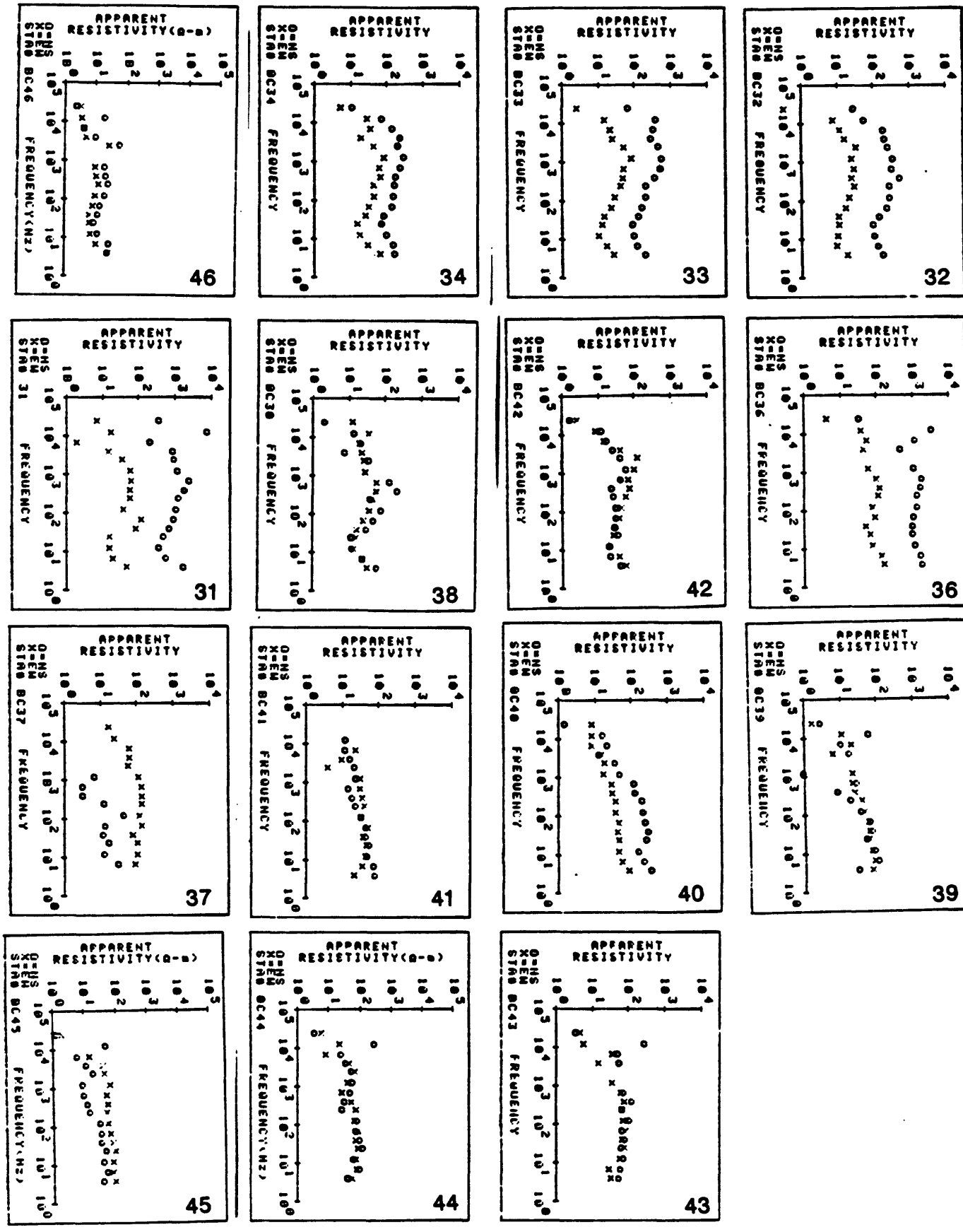

Figure 10--Sounding curves for traverse D-D'.

volcaniclastic rocks, or possibly a weathered zone, at the base of the Bearwallow Mountain Andesite. Considerable separation of the minimum and maximum resistivity curves at most of these stations is attributed to near-surface weathering and fractures in the andesitic bedrock.

The resistivity discontinuity at station 36 suggests a fault, wheareas the resistivity high beneath station 36 could represent an intrusion or silicified rock. Such features are characteristic of caldera ring-fracture zones, as demonstrated in this study in the Mogollon mining district by traverses A-A′ and B-B′. However, the geoelectric patterns seen in sections D-D′ are consistent with intruded faults or silicified zones anywhere and are not unique expressions of caldera margins.

Section E-E′ : North Area

AMT traverse E-E′ (stations 48-51) follows Forest Road 153 on the north flank of Bearwallow Mountain (Figure 8), where it is underlain by Bearwallow Mountain Andesite or deeply weathered float. Resistivity cross sections and sounding curves for traverse E-E′ are shown in Figure 11. Access difficulties prevented locating of AMT stations farther south to better tie into traverse D-D′. The sounding curves for stations 48-51 (Figure 11) all have similar form and comparable amplitudes. Resistivities range from about 10 ohm-m near the surface to a maximum of about 160 ohm-m at middle depths, and decrease again at deeper levels. The low, near-surface resistivity limits penetration of the AMT signals to about 1 kilometer.

Resistivity soundings along traverse E-E′ partly resemble soundings in the western part of traverse D-D′. However, a notable difference between the soundings of the two traverses is the lack of evidence for a resistive zone at the deepest levels along E-E′, which could be the result of the shallower penetration of the AMT signals along E-E′. Separation of the minimum and maximum resistivity curves along traverse E-E′ is generally less than for the sounding stations west of station 36 along traverse D-D′. In

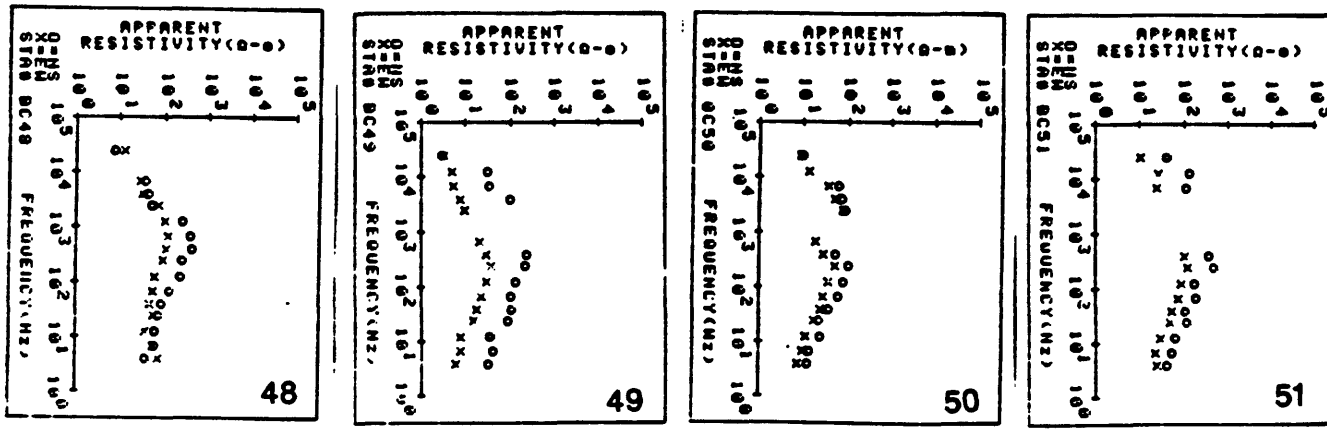

Figure 11--Sounding curves for traverse E-E'.

both areas, the observed separations are interpreted as near-surface effects rather than structural discontinuities in the bedrock. The resistivity soundings and resistivity cross section along traverse E-E′ (Figure 11) show no evidence for a major resistivity discontinuity that might be interpreted to be a significant structural boundary such as a caldera margin. Thus, either the resistivity soundings were unable to detect the caldera margin here or the buried margin of the Bursum caldera probably passes north of the north end of both traverses (D-D′ and E-E′), as approximated by line 1 on Figure 1. This configuration of the northern boundary of the Bursum caldera is consistent with the nearest known outcrops of pre-caldera rocks that can be interpreted to be in the Bursum caldera wall. These include 32.6 Ma dacite and andesite in the Telephone Canyon quadrangle (unpublished geologic map and 40Ar/39Ar age from D.J. Bove) and Bloodgood Canyon Tuff and underlying rhyolite of Elk mountains (equivalent of 28 Ma Taylor Creek Rhyolite) in the southwest corner of the O Bar O Canyon West quadrangle (Richter and Lawrence, 1989). It is also consistent with the inferred northern boundary of the caldera shown on the New Mexico Highway Geologic Map (New Mexico Geological Society, 1982).

CONCLUSIONS

In the southern part of the Mogollon mining district, the geoelectric (AMT) expression of the structural wall and the ring-fracture zone of the Bursum caldera is shown by AMT traverse A-A′ to be characterized by a narrow, deep resistivity high of about 400 ohm m where it coincides with the Queen fault and vein zone.

The high resistivity at the Queen fault and vein zone in the southern part of the district is bordered by nearly symmetrical resistivity lows of less than 100 ohm m, which are interpreted to represent variably propylitically and argillically altered volcanic flows and tuffs of andesitic to rhyolitic composition in the walls of the structure.

Traverse A-A′ also shows a deep zone of high-resistivity

volcanic "basement" rocks of greater than 400 ohm m is inferred to enclose a 5 km wide block of lower resistivity, which may define the extent of the hydrothermal cell beneath the Mogollon district.

AMT traverse B-B′ across the Queen fault zone in the central part of the Mogollon district shows a much weaker and less definitive resistivity high at the fault and vein zone as compared with traverse A-A′.

Traverse C-C′ across the Queen fault in the northern part of the district shows a weak resistivity anomaly whose source and relation to the caldera margin are ambigious.

In the northern region of Busum caldera, AMT traverse D-D′ shows a geoelectric discontinuity that is interpreted as a buried fault zone near the middle of the traverse, west of Negrito Mountain. West of the buried fault, the AMT soundings consistently show a 100-250 ohm-m top layer above a low-resistivity layer of less than 25 ohm-m at a depth of about 200 m, followed by higher resistivity at greater depths. The low- resistivity layer is interpreted as a resistivity discontinuity below the base of the Bearwallow Mountain Andesite.

Northeast of the fault, represented by the resistivity discontinuity along traverse D-D′, the geoelectric section is characterized by monotonically increasing resistivity with depth, which contrasts strongly with the section west of the fault.

A resistivity high at the discontinuity along AMT traverse D-D′ is interpreted as a probable intrusion or silicified rock along the fault. Although the fault and the accompanying intrusion, or silicified rock, inferred by the resistivity patterns along section D-D′ is could mark the buried margin of the Bursum caldera, the evidence is permissible only and requires corroboration by drilling or other means.

AMT soundings along traverse E-E′ show a geoelectric section very similar to that beneath the western part of traverse D-D′, but the soundings along E-E′ did not penetrate deeply enough to verify a lower high-resistivity zone such as is present along D-D′. Traverse E-E′ provides no evidence of a resistivity discontinuity

that can be interpreted as a buried caldera margin. Thus, it seems likely that the northern margin of the Bursum caldera is north of both traverses, D-D'and E-E'. However, the data gap north of Bearwallow Mountain, between the two AMT traverses, allows that the caldera margin passes between the two traverses.

If the caldera margin is north of both AMT traverses, D-D' and E-E', as indicated by this study, then the location of the caldera margin is closely restricted by the nearest outcrops of pre-caldera volcanic rocks north and northeast of this study area, and is remarkably close to the configuration shown on the 1982 New Mexico Geological Society Highway Geologic Map.

Additional AMT soundings are recommended, north and east of this study, to characterize the geoelectric signature of the northern margin of the Bursum caldera.

ACKNOWLEDGEMENTS

John S. Livermore of Public Resource Associates, Inc., and David B. Hackman of Sage Associates, Inc., kindly made available all their data and drill core, which made detailed correlation of geophysical and geologic features in the Mogollon district possible. Richard and Jean Chamberlin of Glenwood, New Mexico, provided valuable assistance. Gerda A. Abrams and Marie-Louise Senterfit assisted in the collection of AMT data.

REFERENCES

Allis, R.G., 1981, Geophysical anomalies over epithermal systems, J. Geochem. Explor., v.36, p.339-374.

Berdichevsky, M.N., and V.I Dimitriev, 1976, Basic principles of interpretation of magnetotelluric sounding curves, in Adam, A., ed., Geoelectric and geothermal studies (east-central Europe, Soviet Asia): Budapest, Akademiai Kiado, KAPG Geophysical Monograph, p.165-221.

Bostick, F.X., Jr., 1977, A simple almost exact method of MT analysis, in Workshop on Evaluation of Electrical Methods in the Geothermal Environment (WEEMGE), Snowbird, Utah, Nov. 1976: University of Utah Report, p.175-177.

Buchanan, L.J., 1981, Precious metal deposits associated with volcanic environments in the southwest, in Dickinson, W.R, and Payne, W.D., eds., Relations of tectonics to ore deposits in the southern Cordillera: Tucson, Arizona Geol. Soc. Digest, 14, p.237-272.

Coney, P.J., 1976, Structure,volcanic stratigraphy and gravity across the Mogollon Plateau, New Mexico: New Mexico Geol. Soc. Special Publication No. 5, p.29-41.

Eggers, D.E. 1982, An eigenstate formulation of the magnetotelluric impedance tensor: Geophysics, 47, p.1,204-1,214.

Ferguson, H.G., 1927, Geology and ore deposits of the Mogollon mining district, New Mexico: U.S.Geological Survey Bull. 787.

Frischknecht, F.C., B.D. Smith, D.B. Hoover, and C.L. Long, 1986, New applications of geoelectrical methods in mineral resource assessment: in Prospects for mineral resource assessments on public lands: proceedings of the Leesburg workshop, U.S. Geol. Surv. Cir 980, p.221-247.

Goldberg, S., and Y. Rotstein, 1982, A simple form of presentation of magnetotelluric data using the Bostick transform: Geophys. Prospecting, 30, p.211-216.

Heald, P., N.K. Foley, and D.O. Hayba, 1987, Comparative anatomy of volcanic-hosted epithermal deposits: acid-sulfate and adularia-sericite types, Econ. Geol., 82, no. 1, p.1-26.

Hoover, D.B., F.C. Frischknecht, and C.L. Tippens, 1976, Audio-magnetotelluric sounding as a reconnaissance exploration technique in Long Valley, California: J. Geophys. Res., 81, no.5, p.801-809.

Hoover, D.B., C.L. Long, and R.M. Senterfit, 1978, Some results from audio-magnetotelluric investigations in geothermal areas: Geophysics, 43, no. 7, p.1,501-1,514.

Houser, B.B. 1981, Geologic map of the Alma quadrangle, Catron County, New Mexico: U.S. Geological Survey map GQ 1610, 1 pl.

Irvine, R.J., M.J. Smith, 1990, Geophysical exploration for epithermal gold deposits, J.of Geochem. Exp. 36, no. 1/3, p.375-412.

Jiracek, G.R., 1990, Near-surface and topographic distortions in electromagnetic induction, in Surveys in Geophysics, 11, No. 2/3, p.163-203.

Keller, G.V., and F.C. Frischknecht, 1966, Electrical methods in geophysical prospecting: Pergamon Press, 519 p.

Long, C.L., 1985, Regional audio-magnetotelluric study of the Questa caldera, New Mexico: J. Geophys. Res, 90, 11,270-11,274.

Marvin, R.F., C.W. Naeser, M. Bikerman, H.H. Mehnert, and J.C. Ratté, 1987, Isotopic ages of post-Paleocene igneous rocks within and bordering the Clifton 1 by 2 quadrangle, Arizona-New Mexico: New Mexico Bureau of Mines and Mineral Resources, Bull. 118.

Mosier, D.L., D.A. Singer, and B.R. Berger, 1986, Descriptive model of Comstock Epithermal veins, Model 25c, 154-157: U.S. Geological Survey Bull. 1693, Mineral Deposit Models, 379 p.

Nelson,P.H., and L.A. Anderson, 1992, Physical properties of ash flow tuff from Yucca Mountain, Nevada: J. Geophys. Res., 97, no.5, p.6,823-6,841.

New Mexico Geological Society, 1982, New Mexico Highway Geologic Map, in cooperation with New Mexico Bureau of Mines and Mineral Resources: Scale 1:1,000,000.

Park, S.K., and D.W. Livelybrooks, 1989, Quantitative interpretation of rotationally invariant parameters in magnetotellurics: Geophysics, 54, p.1,483-1,490.

Ratté, J.C., 1981, Geologic map of the Mogollon quadrangle, Catron County, New Mexico: U.S. Geological Survey GQ 1557, 1 plate.

Ratté,J.C., S.M. Cather, C.E. Chapin, W.A. Duffield, W.E. Elston, and W.C. McIntosh, 1989, Excursion 6a: Eocene-Miocene Mogollon-Datil volcanic field, New Mexico: New Mexico Bureau of Mines and Mineral Resources Memoir 46, p.43-119.

Ratté, J.C., and D.L. Gaskill, 1975, Reconnaissance Geologic Map, Gila Wilderness, New Mexico: U.S. Geological Survey, Miscellaneous Investigations Series Map I-886.

Ratté, J.C., D.L. Gaskill, G.P. Eaton, R.B. Stotelmeyer, and H.C. Meeves, 1979, Mineral Resources of the Gila Primitive Area and Gila Wilderness, Catron and Grant Counties, New Mexico: U.S. Geological Survey Bull. 1451, 229 p.

Ratté, J.C., R.F. Marvin, and C.W. Naeser, 1984, Calderas and ash flow tuffs of the Mogollon Mountains, southwestern New Mexico: J. Geophys. Res. 89, No.B10, p.8,713-8,732.

Ratté, J.C., R.F. Marvin, C.W. Naeser, W.E. Brooks, and T.L Finnell, 1983, Volcanic history of Southwestern Mogollon-Datil volcanic field as recorded along the Morenci lineament, New Mexico and Arizona: Geol. Soc. Amer., Abstracts with programs, 15, No. 5, p.303.

Richter, D.H., and V.A. Lawrence, 1989, Geologic Map of the O Bar O Canyon West Quadrangle: U.S. Geological Survey, Misc. Field Studies Map-MF-2075, Scale 1:24,000.

Senterfit, R.M., and G.A. Abrams, 1991, Audiomagnetotelluric investigation at Bursum caldera, Mogollon mining district, west central New Mexico: location map and data report, U.S. Geological Survey Open-file Rep. 91-624, 30 p., 1 plate.

Senterfit, R.M., and D.P. Klein, 1992, Audio-magnetotelluric investigation at Turkey Creek caldera, Chiricahua mountains, southeastern Arizona, Chapter K in Thorman, C.H., ed., Application of structural geology to mineral and energy resources of the central and western United States, U.S. Geological Survey Bull. 2012.

Strangway, D.W., C.M. Swift,Jr., and R.C. Holmer, 1973, The application of audio-frequency magnetotellurics (AMT) to mineral exploration: Geophysics, 38, no. 6, p.1,159-1,175.

Strangway, D.W., and A. Kozier, 1979, Audio-frequency magnetotelluric sounding - a case history at the Cavendish geophysical test range: Geophysics, 44, no. 8, p.1,429-1,446.

Vozoff, K., 1972, The magnetotelluric method in the exploration of sedimentary basins: Geophysics, 37, no.1, p.98-141.

Weidelt, P., 1972, The inverse problem of geomagnetic induction: Journal of Geophysics, 38, p.257-289.